Formulation and Comparison of Two Detectors of Independent Timing Jitter in a Complex Harmonic

Mark R. Morelande and D. Robert Iskander, *Member, IEEE*

***Abstract*—Two detectors of symmetrically distributed independent timing jitter in a data record composed of a complex harmonic in additive white Gaussian noise are proposed. The proposed detectors are computationally efficient, and although they are formulated using asymptotic results, they may be effectively used with small sample lengths under a wide range of conditions. The conditions required for consistency of the detectors are derived and examined for important special cases. The performances of the detectors are analyzed using simulations.**

***Index Terms*—Complex harmonic, detection, timing jitter.**

I. Introduction

NEARLY all sampling systems are prone to timing jitter wherein the spacing between sampling instants is not uniform but varies about the nominal sampling period in a random fashion. Defects in the sampling system such as corruption of the sampling pulse with noise and instabilities in the sampling clock are common causes of timing jitter [1], [3]. Timing jitter may also be an unavoidable part of the data collection such as in the estimation of upper atmospheric tides from the radar echoes of meteors [4] or in sonar [14], where sensor motion is equivalent to timing jitter. In many cases, the deviations from the nominal sampling period are small enough that they may be ignored. However, there are instances in which the effects of jitter can become significant. The aim of this paper is to detect such instances. The signal model considered here is a complex harmonic in additive noise that may or may not have randomly spaced sampling instants. Specifically, we consider observations from

$$X_t = g_0 \exp[j\{\omega_0(t+U_t)+\psi\}] + W_t, \quad t \in \mathbb{Z} \qquad (1)$$

where $g_0 \in \mathbb{R}^+, -\pi \leq \omega_0 < \pi, \omega_0 \neq 0, -\pi \leq \psi < \pi, U_t, t \in \mathbb{Z}$ are zero-mean real-valued independent and identically distributed (iid) random variables with variance σ_U^2, and $\{W_t\}$ is a circular complex-valued white normal random process with variance σ_W^2, independent of $\{U_t\}$. It is assumed that $\{U_t\}$ is symmetrically distributed with characteristic function $\phi_U(s) = \mathsf{E}\exp(jsU_t)$ for $s \in \mathbb{R}$. Throughout this paper, realizations, or observations, of a random process are referred to using lower case notation, e.g., $u_0, \ldots, u_{n-1}$ are a set of observations of the random process $\{U_t\}$.

We aim to provide a solution to the following problem: Given observations $x_0, \ldots, x_{n-1}$ from (1), test the hypothesis H : $\sigma_U = 0$ against the alternative K : $\sigma_U > 0$. Under this formulation, a decision for the alternative indicates the presence of timing jitter. It is assumed that all signal and noise parameters and the values $u_0, \ldots, u_{n-1}$ of the timing offsets are unknown. Note that throughout the paper, it will be implicitly assumed that σ_U^2 is finite, although this is not strictly necessary. The only conditions on the jitter process are that it is iid and symmetrically distributed. When considering jitter distributions with infinite variance, σ_U^2 may be replaced as an appropriate scale parameter.

Our consideration of the jitter detection problem was motivated by our experiences in measuring the dynamics of wavefront aberration in the human eye. The wavefront error of an eye can be measured with a Hartmann–Shack sensor [6]. This is an optical instrument equipped with a laser, an array of small lenses, and a CCD video camera. The light reflects from the retina, passes through the array of lenses, and forms an image that falls on the CCD. The displacements in the grid image from the ideal square grid are used to calculate transversal aberrations, which are related to the wavefront error. Traditionally, such measurements have been performed in a static manner (single measurement). In order to gain a better understanding of the human vision system, recent studies have considered measurement of the dynamics of the wavefront aberration [5]. Consecutive measurements indicate that the wavefront aberration varies in a sinusoidal fashion through time. However, an accurate analysis is complicated by the fact that the sampling period seems to vary from one measurement to the next as a result of the rudimentary nature of the sampling systems in commercially available wavefront sensors. The techniques of this paper were developed to provide a formal framework to test this supposition. More generally, a method of checking for the presence of timing jitter is desirable as a diagnostic tool for evaluating the performance of sampling systems. A jitter detector can also be used to select a suitable estimation procedure since the optimal estimation procedure will differ depending on whether or not jitter exists.

Previous work on detecting timing jitter has been performed by Sharfer and Messer [9], [10]. In that case, the presence of jitter in the sampling of a bandlimited zero-mean stationary random process with nonzero third-order cumulants was found to be characterized by non-nullity of the bispectrum in a certain region. This observation precipitated the formulation of an

Manuscript received June 22, 2001; revised April 10, 2003. The associate editor coordinating the review of this paper and approving it for publication was Dr. Ta-Hsin Li.

M. R. Morelande is with the CRC for Sensor Signal and Information Processing, Department of Electrical and Electronic Engineering, The University of Melbourne, Parkville, VIC 3010, Australia (e-mail: m.morelande@ee.mu.oz.au).

D. R. Iskander is with the Centre for Health Research (Optometry), Queensland University of Technology, Kelvin Grove, Q4059, Australia (e-mail: d.iskander@qut.edu.au).

Digital Object Identifier 10.1109/TSP.2003.818901

appropriate statistical test. The bispectrum jitter detector cannot be used for the problem considered here because the random process $\{X_t\}$ of (1) does not satisfy the required assumptions. No jitter detectors for the signal model considered here have been proposed in the literature, although various authors have examined the effect of jitter on sinusoids. For example, the signal-to-noise ratio (SNR) of a sinusoid with timing jitter was analyzed in [1], [2], and [13], approximate CRB's for the signal and noise parameters were derived in [11], the periodogram of a complex harmonic with timing jitter was studied in [3], and a jitter variance estimator was proposed in [12] for the case of a real-valued sinusoid with known amplitude, frequency, and initial phase.

In this paper, two detectors that use test statistics based on estimators of $\omega_0^2\sigma_U^2$ are proposed. Starting from the same result, the test statistics are derived using different assumptions. In the first case, the jitter is assumed to be normally distributed, whereas in the second case, a small jitter assumption is made. The resulting detectors are computationally efficient and are consistent under mild conditions on the characteristic function of the jitter process. Although the detectors are derived using asymptotic results, it is shown that the small jitter assumption detector maintains the nominal false alarm probability in all cases, whereas the normal assumption detector does so under moderate conditions on the SNR.

The paper is structured as follows. The detectors are formulated, and the conditions under which they are consistent are established in Section II. Section III contains a performance analysis using theoretical and simulation results. The paper concludes with a summary of the main results.

II. Proposed Methods

In this section, two detectors of independent timing jitter are proposed. The conditions under which the detectors are consistent are established and examined for various jitter distributions. For the sake of convenience, it is assumed during the analysis that $\sigma_U^2 < \infty$, although this is not necessary.

After estimating the frequency ω_0 and initial phase ψ as

$$\hat{\omega}_0 = \arg \max_{-\pi \le \omega < \pi} |d_X(\omega)| \tag{2}$$

$$\hat{\psi} = \angle d_X(\hat{\omega}_0) \tag{3}$$

where $d_X(\omega)$ is the finite Fourier transform (FT) of $x_0, \ldots, x_{n-1}$

$$d_X(\omega) = \sum_{t=0}^{n-1} x_t \exp(-j\omega t)$$

the observations are demodulated to form the sequence

$$y_t = x_t \exp\{-j(\hat{\omega}_0 t + \hat{\psi})\}, \quad t = 0, \ldots, n-1. \tag{4}$$

Under the given assumptions, it is shown in Appendix A that $\hat{\omega}_0 = \omega_0 + O_m(n^{-3/2})$ and $\hat{\psi} = \psi + O_m(n^{-1/2})$, where, for a sequence of random variables $\{\varepsilon_n\}$ and a sequence of positive real numbers $\{a_n\}$, the notation $\varepsilon_n = O_m(a_n)$ means that $\mathsf{E}|\varepsilon_n/a_n|^k \le c_k, k = 1, 2, \ldots$ for all n, where c_k is a positive constant. It follows that $y_0, \ldots, y_{n-1}$ are observations from the random process

$$\begin{aligned} Y_t &= X_t \exp\{-j(\omega_0 t + \psi)\} + O_m(n^{-1/2}) \\ &= g_0 \exp(j\xi_t) + V_t + O_m(n^{-1/2}), \quad t = 0, \ldots, n-1 \end{aligned} \tag{5}$$

where $\xi_t = \omega_0 U_t$, and $V_t = W_t / \exp\{j(\omega_0 t + \psi)\}$. Since it is assumed that $\omega_0 \neq 0$, the variance σ_ξ^2 of $\{\xi_t\}$ will be zero only if $\sigma_U^2 = 0$. Therefore, non-nullity of σ_ξ^2 can be used to test for the presence of jitter.

In the following, terms in (5) that disappear as the sample length $n \to \infty$ will be ignored, i.e., we proceed with $Y_t = g_0 \exp(j\xi_t) + V_t$. Let $r_{kY} = \mathsf{E}[\{\mathrm{Re}(Y_t)\}^k]$ and $i_{kY} = \mathsf{E}[\{\mathrm{Im}(Y_t)\}^k]$ for $k = 1, 2, \ldots$. For convenience, we write $r_Y = r_{1Y}$ and $i_Y = i_{1Y}$. It is straightforward to show that under the assumption of symmetrically distributed jitter

$$\sqrt{r_{2Y} - i_{2Y}}/r_Y = \sqrt{\phi_\xi(2)}/\phi_\xi(1) \tag{6}$$

where $\phi_\xi(s) = \mathsf{E}\exp(js\xi_t)$ is the characteristic function of $\{\xi_t\}$. Since $\phi_\xi(s)$ is a function of σ_ξ^2, knowledge of the functional form of $\phi_\xi(s)$ enables the formulation of an unbiased estimator of σ_ξ^2 using (6). In particular, we can replace $\phi_\xi(s)$ by its functional form, replace the moments by sample estimators, and solve for σ_ξ^2. Since the jitter distribution is assumed to be unknown, the functional form of $\phi_\xi(s)$ is not available, and an estimator of σ_ξ^2, which is, in general, unbiased, cannot be obtained from (6). However, since the aim of this paper is to *detect* jitter, the basic requirement is a test statistic that will tend toward higher values under the alternative compared to the null. Of course, this basic requirement does not guarantee a practical detector, and it is usually necessary for the test statistic to possess desirable properties that will lead to a consistent detector with high detection probabilities under the alternative. The important point, however, is that unbiasedness is not a necessity for the purposes of jitter detection. With this in mind, one approach is to assume a distribution for the jitter and derive an estimator of σ_ξ^2 on this basis. Another approach is to assume small amounts of jitter and replace the characteristic function $\phi_\xi(s)$ by its second-order approximation. A distribution-independent estimator can then be derived. Both of these approaches require that the performances of the resulting detectors are carefully studied for a range of jitter distributions. This analysis will be performed in Section III.

A. Normal Assumption

We will proceed from (6) as if the jitter is normally distributed. The normal distribution is chosen for the simple derivation it affords. This does not prohibit the use of the proposed detector for other jitter distributions, as will be demonstrated in Section III. Substituting $\phi_\xi(s) = \exp(-s^2\sigma_\xi^2/2)$ into (6) gives

$$\exp(-\sigma_\xi^2/2) = \sqrt{r_{2Y} - i_{2Y}}/r_Y.$$

Simple rearrangements result in the following:

$$\sigma_\xi^2 = 2\log(r_Y/\sqrt{r_{2Y} - i_{2Y}}).$$

Since the moments of the real and imaginary parts of $\{Y_t\}$ are unavailable, they are replaced by their sample estimators

$$\hat{r}_{kY} = 1/n \sum_{t=0}^{n-1} \{\mathrm{Re}(Y_t)\}^k \tag{7}$$

$$\hat{\imath}_{kY} = 1/n \sum_{t=0}^{n-1} \{\mathrm{Im}(Y_t)\}^k \tag{8}$$

with $\hat{r}_Y = \hat{r}_{1Y}$ and $\hat{\imath}_Y = \hat{\imath}_{1Y}$ to form the estimator

$$\begin{aligned}\hat{\sigma}_\xi^2 &= 2\log(\hat{r}_Y/\sqrt{\hat{r}_{2Y} - \hat{\imath}_{2Y}}), \\ &= \log\left\{\hat{r}_Y^4/(\hat{r}_{2Y} - \hat{\imath}_{2Y})^2\right\}/2. \end{aligned} \tag{9}$$

Negative values of the variance estimate (9) arise when the true value of σ_ξ^2 is close to zero. While negative variance values cannot strictly be interpreted, we can provide a rough interpretation by noting that when negative variance estimates occur, the test statistic $\hat{T}$, which will be defined below, will be lower than the threshold so that the null hypothesis is accepted. Thus, negative variance estimates can be interpreted as meaning that the true jitter variance is zero, i.e., no jitter is present. Note that (9) should be used instead of the previous line when computing $\hat{\sigma}_\xi^2$ since otherwise, the argument of the logarithm will be complex-valued when $\hat{r}_{2Y} - \hat{\imath}_{2Y} < 0$. We show in Appendix C that $\hat{\boldsymbol{\theta}} = (\hat{r}_Y, \hat{\imath}_{2Y}, \hat{r}_{2Y})'$ has the asymptotic distribution

$$\sqrt{n}(\hat{\boldsymbol{\theta}} - \boldsymbol{\mu}_{\hat{\boldsymbol{\theta}}}) \overset{a}{\sim} \mathsf{N}(0, \boldsymbol{\Sigma}_{\hat{\boldsymbol{\theta}}}) \tag{10}$$

where the elements of $\boldsymbol{\mu}_{\hat{\boldsymbol{\theta}}} = \mathsf{E}\hat{\boldsymbol{\theta}}$ are given in (42)–(44), and the elements of $\boldsymbol{\Sigma}_{\hat{\boldsymbol{\theta}}} = n\mathsf{E}(\hat{\boldsymbol{\theta}} - \boldsymbol{\mu}_{\hat{\boldsymbol{\theta}}})(\hat{\boldsymbol{\theta}} - \boldsymbol{\mu}_{\hat{\boldsymbol{\theta}}})'$ are given in (45)–(50). Using (10) and [8, Th. 3.3.A], it can be shown that under H, $\sqrt{n}\hat{\sigma}_\xi^2 \overset{a}{\sim} \mathsf{N}(0, \sigma_W^4/g_0^4)$. Under the null hypothesis, consistent estimators of g_0 and σ_W^2 are given by $\hat{r}_Y$ and $2\hat{\imath}_{2Y}$, respectively. We therefore propose the normalized test statistic $\hat{T} = \sqrt{n}\hat{r}_Y^2\hat{\sigma}_\xi^2/(2\hat{\imath}_{2Y})$. Using [8, Th. 3.3.A.], we have that for $\phi_\xi(s) \neq 0, s = 1, 2$

$$\hat{T} - \mu_{\hat{T}} \overset{a}{\sim} \mathsf{N}\left(0, \sigma_{\hat{T}}^2\right) \tag{11}$$

where

$$\mu_{\hat{T}} = \hat{T}|_{\hat{\boldsymbol{\theta}} = \boldsymbol{\mu}_{\hat{\boldsymbol{\theta}}}} = \sqrt{n}\frac{\phi_\xi(1)^2 \log\{\phi_\xi(1)^4/\phi_\xi(2)^2\}}{2\{1 - \phi_\xi(2) + 1/\mathcal{S}\}} \tag{12}$$

and $\sigma_{\hat{T}}^2 = \boldsymbol{d}'\boldsymbol{\Sigma}_{\hat{\boldsymbol{\theta}}}\boldsymbol{d}$ with

$$\begin{aligned}\boldsymbol{d} &= \frac{1}{\sqrt{n}}\nabla_{\hat{\boldsymbol{\theta}}}\hat{T}|_{\hat{\boldsymbol{\theta}} = \boldsymbol{\mu}_{\hat{\boldsymbol{\theta}}}} \\ &= \begin{pmatrix} \frac{g_0\phi_\xi(1)[\log\{\phi_\xi(1)^4/\phi_\xi(2)^2\}+2]}{g_0^2\{1-\phi_\xi(2)\}+\sigma_W^2} \\ \frac{\phi_\xi(1)^2}{g_0^2\{1-\phi_\xi(2)\}+\sigma_W^2}\left[\frac{1}{\phi_\xi(2)} - \frac{\log\{\phi_\xi(1)^4/\phi_\xi(2)^2\}}{1-\phi_\xi(2)+1/\mathcal{S}}\right] \\ -\frac{\phi_\xi(1)^2}{\phi_\xi(2)\left[g_0^2\{1-\phi_\xi(2)\}+\sigma_W^2\right]} \end{pmatrix} \end{aligned} \tag{13}$$

where $\nabla_{\hat{\boldsymbol{\theta}}} = (\partial/\partial\hat{r}_Y, \partial/\partial\hat{\imath}_{2Y}, \partial/\partial\hat{r}_{2Y})'$. Although (11) is asymptotically correct if $\phi_\xi(1)$ and $\phi_\xi(2)$ are nonzero, for small sample lengths $n < 1000$, the asymptotic approximation is poor when ω_0, and the parameters of the jitter process are such that either $\phi_\xi(1)$ or $\phi_\xi(2)$ are close to zero. Under the null, $\phi_\xi(s) = 1, \forall s$ so that $\mu_{\hat{T}} = 0$, and

$$\begin{aligned}\boldsymbol{d} &= (2g_0, 1, -1)'/\sigma_W^2, \\ \boldsymbol{\Sigma}_{\hat{\boldsymbol{\theta}}} &= \sigma_W^2 \begin{pmatrix} 1/2 & 0 & g_0 \\ 0 & \sigma_W^2/2 & 0 \\ g_0 & 0 & 2g_0^2 + \sigma_W^2/2 \end{pmatrix}. \end{aligned} \tag{14}$$

It follows that $\boldsymbol{d}'\boldsymbol{\Sigma}_{\hat{\boldsymbol{\theta}}}\boldsymbol{d} = 1$ and $\hat{T} \overset{a}{\sim} \mathsf{N}(0, 1)$ under H. We therefore reject the null hypothesis, i.e., decide for the presence of jitter, if $\hat{T} > \Phi^{-1}(1 - \alpha)$, where $\Phi(\cdot)$ is the standard normal distribution function, and α is the prescribed false alarm probability. The detection probability can then be found as

$$\beta_{\hat{T}} = 1 - \Phi[\{\Phi^{-1}(1 - \alpha) - \mu_{\hat{T}}\}/\sigma_{\hat{T}}]. \tag{15}$$

The jitter detector obtained by testing $\hat{T}$ will be termed the normal assumption (NA) detector. Note that scaling $\hat{\sigma}_\xi^2$ by $\sqrt{n}\hat{r}_Y^2/(2\hat{r}_{2Y})$ would also lead to a test statistic that is asymptotically standard normal under H. However, this formulation would result in a detector with reduced power since, in most cases, $\hat{r}_{2Y}$ tends to take on larger values than $\hat{\imath}_{2Y}$ under the alternative.

B. Small Jitter Approximation

Before applying the small jitter approximation, we square both sides of (6) to obtain

$$(r_{2Y} - \imath_{2Y})/r_Y^2 = \phi_\xi(2)/\phi_\xi(1)^2. \tag{16}$$

Under the small jitter approximation and assuming symmetrically distributed jitter, $\phi_\xi(s) = 1 - s^2\sigma_\xi^2/2$ is substituted into (16), giving

$$\begin{aligned}(r_{2Y} - \imath_{2Y})/r_Y^2 &\approx \left(1 - 2\sigma_\xi^2\right)\Big/\left(1 - \sigma_\xi^2/2\right)^2 \\ &\approx \left(1 - 2\sigma_\xi^2\right)\left(1 + \sigma_\xi^2\right) \qquad (17) \\ &\approx 1 - \sigma_\xi^2 \qquad (18) \end{aligned}$$

where (17) is obtained by replacing the denominator on the right-hand side with its first-order Taylor series approximation, and (18) follows from (17) by retaining only first-order terms. Equation (18) leads to the approximation $\sigma_\xi^2 \approx 1 - (r_{2Y} - \imath_{2Y})/r_Y^2$. Replacing the moments with their sample estimators (7) and (8) results in the following estimator of σ_ξ^2:

$$\tilde{\sigma}_\xi^2 = 1 - (\hat{r}_{2Y} - \hat{\imath}_{2Y})/\hat{r}_Y^2\,. \tag{19}$$

The remarks following (9) regarding the negativity of $\hat{\sigma}_\xi^2$ for small values of σ_ξ^2 also apply to $\tilde{\sigma}_\xi^2$. Note that there are several ways in which the small jitter approximation may be employed to arrive at an approximate expression for the jitter variance. The method we have chosen here results in the best performance in terms of maintaining the nominal false alarm probability as well as achieving a high detection probability under the alternative. In Appendix B, we present a brief discussion on the properties of the competing small jitter approximations. We also show why the variance estimator proposed in [12] for the real-valued case under a small jitter assumption cannot be extended to the complex-valued case.

Although $\tilde{\sigma}_\xi^2$ is, in general, a biased estimator of σ_ξ^2, it is asymptotically unbiased when $\sigma_U^2 = 0$, i.e., $\mathsf{E}\tilde{\sigma}_\xi^2 = 0$ under H. Using [8, Th. 3.3.A] and (10), it can be shown that under H, $\sqrt{n}\tilde{\sigma}_\xi^2 \overset{a}{\sim} \mathsf{N}(0, \sigma_W^4/g_0^4)$. It is not surprising to see that the asymptotic null distribution of $\tilde{\sigma}_\xi^2$ is the same as that of $\hat{\sigma}_\xi^2$. Standardization leads to the test statistic $\tilde{T} = \sqrt{n}\hat{r}_Y^2\tilde{\sigma}_\xi^2/(2\hat{\imath}_{2Y})$, which, after substituting (19), can be written as

$$\tilde{T} = \sqrt{n}\left(\hat{r}_Y^2 - \hat{r}_{2Y} + \hat{\imath}_{2Y}\right)/\left(2\hat{\imath}_{2Y}\right).$$

It follows from [8, Th. 3.3.A.] that

$$\tilde{T} - \mu_{\tilde{T}} \overset{a}{\sim} \mathsf{N}(0, \sigma_{\tilde{T}}^2)$$

where

$$\mu_{\tilde{T}} = \tilde{T}|_{\hat{\boldsymbol{\theta}}=\boldsymbol{\mu}_{\hat{\boldsymbol{\theta}}}} = \sqrt{n}\frac{\phi_\xi(1)^2 - \phi_\xi(2)}{1 - \phi_\xi(2) + 1/\mathcal{S}} \tag{20}$$

and $\sigma_{\tilde{T}}^2 = \boldsymbol{h}'\boldsymbol{\Sigma}_{\hat{\boldsymbol{\theta}}}\boldsymbol{h}$ with

$$\begin{aligned}\boldsymbol{h} &= \frac{1}{\sqrt{n}}\nabla_{\hat{\boldsymbol{\theta}}}\tilde{T}|_{\hat{\boldsymbol{\theta}}=\boldsymbol{\mu}_{\hat{\boldsymbol{\theta}}}} \\ &= \begin{pmatrix} \frac{2g_0\phi_\xi(1)}{g_0^2\{1-\phi_\xi(2)\}+\sigma_W^2} \\ -\frac{g_0^2[2\phi_\xi(1)^2-\{1+\phi_\xi(2)+1/\mathcal{S}\}]}{\left[g_0^2\{1-\phi_\xi(2)\}+\sigma_W^2\right]^2} \\ -1/\left[g_0^2\{1-\phi_\xi(2)\}+\sigma_W^2\right] \end{pmatrix}.\end{aligned} \tag{21}$$

Under the null, $\boldsymbol{h} = (2g_0, 1, -1)'/\sigma_W^2$, and it follows from using (14) that $\boldsymbol{h}'\boldsymbol{\Sigma}_{\hat{\boldsymbol{\theta}}}\boldsymbol{h} = 1$ and $\tilde{T} \overset{a}{\sim} \mathsf{N}(0,1)$. Therefore, H is rejected if $\tilde{T} > \Phi^{-1}(1-\alpha)$. The detection probability of the small jitter approximation detector is, for large n

$$\beta_{\tilde{T}} = 1 - \Phi[\{\Phi^{-1}(1-\alpha) - \mu_{\tilde{T}}\}/\sigma_{\tilde{T}}]. \tag{22}$$

The jitter detector obtained by testing $\tilde{T}$ will be termed the small jitter approximation (SJA) detector.

In the following subsection, the conditions required for consistency of the SJA and NA detectors are explored for several jitter distributions.

C. Consistency

It can be seen from (20) and (22) that the SJA detector will be consistent, i.e., the detection probability tends to one as $n \to \infty$ for fixed parameter values, if

$$\phi_\xi(1)^2 > \phi_\xi(2). \tag{23}$$

It follows from (12) and (15) that consistency of the NA detector requires

$$\phi_\xi(1)^4 > \phi_\xi(2)^2. \tag{24}$$

Note that conditions (23) and (24) are equivalent only if $\phi_\xi(2) > 0$ for all values of the parameters ω_0 and σ_U^2. The conditions (23) and (24) will be explored for normal, uniform, and alpha-stable jitter distributions.

In the case of normally distributed jitter, $\phi_\xi(s) > 0, \forall s$, and all values of $\sigma_\xi^2 = \omega_0^2\sigma_U^2$; therefore, the conditions required for consistency of the SJA and NA detectors are identical. Letting $\phi_\xi(s) = \exp(-s^2\omega_0^2\sigma_U^2/2)$ in (23) gives

$$\phi_\xi(1)^2 = \exp\left(-\omega_0^2\sigma_U^2\right) > \phi_\xi(2) = \exp\left(-2\omega_0^2\sigma_U^2\right)$$

for all values of $\omega_0 \in [-\pi, \pi), \omega_0 \neq 0$, and $\sigma_U^2 > 0$. Therefore, the proposed detectors are consistent detectors of normally distributed jitter for all jitter variances and signal frequencies.

For uniformly distributed jitter, $U_t \sim \mathsf{U}(-a, a), a > 0$, the characteristic function $\phi_\xi(s) = \sin(s\omega_0 a)/(s\omega_0 a)$, and (23) becomes

$$\tan(\omega_0 a)/(\omega_0 a)\begin{cases} >1, & \sin(2\omega_0 a)/(2\omega_0 a) > 0 \\ <1, & \sin(2\omega_0 a)/(2\omega_0 a) < 0. \end{cases} \tag{25}$$

Since

$$\sin(2\omega_0 a)/(2\omega_0 a)\begin{cases} >0, & k\pi \le |\omega_0| a < (k+1/2)\pi, \quad k = 0, 1, \ldots \\ <0, & (k+1/2)\pi \le |\omega_0| a < (k+1)\pi, \quad k = 0, 1, \ldots \end{cases}$$

we obtain the following conditions required for consistency of the SJA detector in the presence of uniformly distributed jitter:

$$\tan(\omega_0 a)/(\omega_0 a)\begin{cases} >1, & k\pi \le |\omega_0| a < (k+1/2)\pi, \quad k = 0, 1, \ldots \\ <1, & (k+1/2)\pi \le |\omega_0| a < (k+1)\pi, \quad k = 0, 1, \ldots \end{cases} \tag{26}$$

Similar computations yield the conditions required for consistency of the NA detector in the presence of uniformly distributed jitter as

$$|\tan(\omega_0 a)/(\omega_0 a)| > 1. \tag{27}$$

Equations (26) and (27) can be used to show that in the presence of uniformly distributed jitter, the SJA detector is consistent under a wider range of conditions than the NA detector. However, for practical applications, it is important to note that both detectors are consistent for $|\omega_0| a \le 2$. When $|\omega_0| a > 2$, we have that $a > 4/\pi$, which is a level of jitter that would rarely be encountered in practice. Therefore, the more general consistency of the SJA detector in the presence of uniformly distributed jitter is of questionable practical importance.

It is interesting to consider the case where U_t has a symmetric alpha-stable distribution with characteristic exponent a and dispersion γ. The characteristic function of the jitter process is $\phi_\xi(s) = \exp(-\gamma|s\omega_0|^a)$, and it is straightforward to show that the inequalities (23) and (24) are satisfied if $a > 1$. In this case, $\hat{\sigma}_\xi^2$ and $\tilde{\sigma}_\xi^2$ cannot be regarded as estimators of σ_ξ^2 since the variance of an alpha-stable random variable is infinite. Rather, $\hat{\sigma}_\xi^2$ and $\tilde{\sigma}_\xi^2$ are estimators of $2\gamma|\omega_0|^a$. Although the suitability of the alpha-stable distribution for modeling jitter is disputable, this result does underline the robustness of the proposed detectors.

III. Performance Analysis

This section contains a performance analysis and comparison of the proposed jitter detectors. Since the detectors are formulated using asymptotic results, it is first necessary to verify their

TABLE I
ESTIMATED FALSE ALARM PROBABILITIES (IN PERCENT) FOR THE SJA (LEFT) AND NA (RIGHT) JITTER DETECTORS. SNR = 0 DB

	α (%)			
$\log_2(n)$	1		5	
5	0	0.43	0.69	2.99
6	0.02	0.41	1.62	3.24
7	0.14	0.53	2.51	3.81
8	0.31	0.70	3.10	3.90
9	0.47	0.68	3.71	4.32
10	0.60	0.79	3.95	4.36
11	0.74	0.88	4.29	4.61

ability to maintain the prescribed false alarm probability for finite data records. In the second part of this section, the performances of the detectors are analyzed for normal and uniform jitter distributions. The final part of this section addresses the problem of finding the sample length required for adequate performance under given conditions.

A. False Alarm Probability

The false alarm probabilities of the jitter detectors are estimated for various sample lengths and nominal false alarm probabilities of 1 and 5%. The frequency $\omega_0 = 1$, the initial phase $\psi = 1/2$, and the SNR $= g_0^2/\sigma_W^2$ is set to 0 dB. For each scenario, 50 000 realizations of (1) are generated under the null hypothesis. The results, which are shown in Table I, indicate that both detectors maintain the nominal false alarm probability in all cases. Although both detectors are excessively conservative for small sample lengths, it can be seen that the actual false alarm probabilities approach the nominal false alarm probabilities as the sample length increases.

It is interesting to examine the effect of SNR on the ability of the detectors to maintain the nominal false alarm probability. Fig. 1 shows plots of the empirical false alarm probabilities of the two detectors against SNR for $n = 128, 512$, and $\alpha = 0.01, 0.05$. For each scenario, 50 000 realizations are used to obtain the empirical results. It is evident that the NA detector does not maintain the nominal false alarm probability for all SNRs. However, this is not a great disadvantage since the detector fails to maintain the set level only for SNRs below -3 dB. Interestingly, the threshold SNR of -3 dB is approximately the same for $n = 128$ and $n = 512$, although the empirical false alarm probability is much closer to the nominal false alarm probability for the larger sample length. Additional simulation results, which are not reported here for the sake of brevity, show that this trend subsists as the sample length n increases. The SJA detector has the desirable property that its empirical false probability is approximately constant and below the nominal false probability for all SNRs.

B. Detection Probability

The powers of the two detectors are now examined. In the first example, the jitter is normally distributed. Note that the performances of the detectors are determined by the values of the SNR $= g_0^2/\sigma_W^2$ and $\sigma_\xi^2 = \omega_0^2\sigma_U^2$. Thus, an increase in ω_0 has the same effect as an increase in σ_U. In the following simulations, we will fix the signal frequency ω_0 and amplitude g_0 and vary the jitter variance σ_U^2 and additive noise variance σ_W^2. The same results could be obtained by keeping σ_U^2 constant and varying ω_0 (as long as $\omega_0 \in [-\pi, \pi)$), or even varying both quantities, and similarly for g_0 and σ_W^2. The variance $\sigma_\xi^2 = \omega_0^2\sigma_U^2$ is varied between 10^{-3} and 1 with $\omega_0 = 1$. The initial phase $\psi = 1/2$, and the sample length $n = 512$. Simulation results obtained using 5000 realizations of (1) for each scenario are shown in Figs. 2 and 3 for SNRs of 10 and 0 dB, respectively. In each case, false alarm probabilities of $\alpha = 0.01$ and $\alpha = 0.05$ are considered. For an SNR of 10 dB, it can be seen that both detectors achieve high detection probabilities for small values of σ_ξ^2. This is not the case for SNR $= 0$ dB. Indeed, the detection probabilities actually decrease as σ_ξ^2 increases beyond about $1/2$. Additional simulations, which are not shown here, verify that for a given SNR, this effect disappears as the sample length n increases.

For SNR $= 10$ dB, it is evident that the performances of the two detectors are identical. This happens because in the region where it is expected that significant differences in the properties of the test statistics will occur, i.e., $\sigma_\xi^2 > 1/4$, the mean values of both test statistics are well within the acceptance region, and therefore, the bias of the small jitter approximation has no effect on the detection probability. Differences in the performances of the two detectors can be discerned for SNR $= 0$ dB. In particular, the NA detector achieves a higher detection probability than the SJA detector for all values of σ_ξ^2 with a larger increase in performance, which is evident for the smaller false alarm probability $\alpha = 0.01$. Even so, it is interesting to note that the performance of the SJA detector closely approaches that of the NA detector under conditions that are much different from those under which it was formulated.

The above simulations are repeated using uniformly distributed jitter with the results shown in Figs. 4 and 5. Once again, the detectors perform identically for SNR $= 10$ dB. For an SNR of 0 dB, the NA detector has a higher detection probability for moderate values of σ_ξ^2, but a sudden decrease in its detection probability is evident for σ_ξ^2 close to one. A similar drop in performance can be shown to exist for the SJA detector, although this does not occur until $\sigma_\xi^2 \geq 2$. Therefore, the SJA detector is a more robust detector of uniformly distributed jitter than the NA detector. These observations are more likely to be of theoretical rather than practical interest as it does not seem reasonable to expect values of σ_ξ^2 beyond $1/4$ in practice.

In summary, for normally distributed jitter, the NA detector performs slightly better than the SJA detector for all values of the SNR and σ_ξ^2, with the difference in performance increasing as the SNR and/or α decrease. In the presence of uniformly distributed jitter, the NA detector has superior performance in moderate conditions, whereas the SJA detector is more robust and can still operate in extreme conditions, i.e., large σ_ξ^2 and low SNR, under which the NA detector fails. The enhanced robustness of the SJA detector is of debatable importance, considering that it is unlikely that extremely large values of σ_ξ^2 would be encountered in practice.

C. Sample Length Requirements

It is of interest to determine the sample length required to achieve a certain detection probability under given conditions.

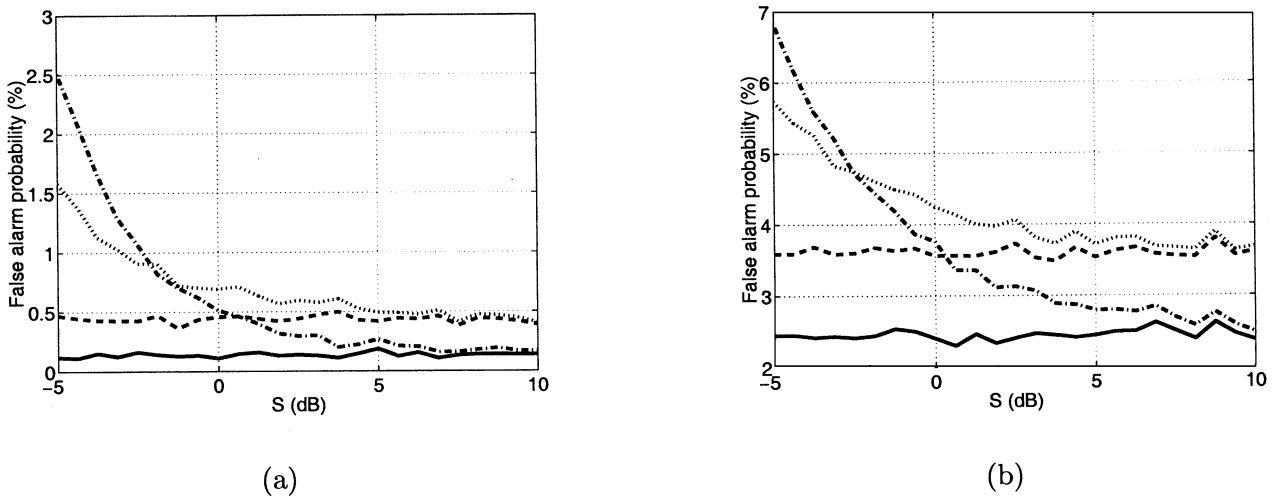

Fig. 1. Empirical false alarm probability (in percent) plotted against SNR (in decibels) for (a) $\alpha = 0.01$ and (b) $\alpha = 0.05$. Results are shown for the SJA detector for $n = 128$ (solid) and $n = 512$ (dashed) and the NA detector for $n = 128$ (dash-dot) and $n = 512$ (dotted).

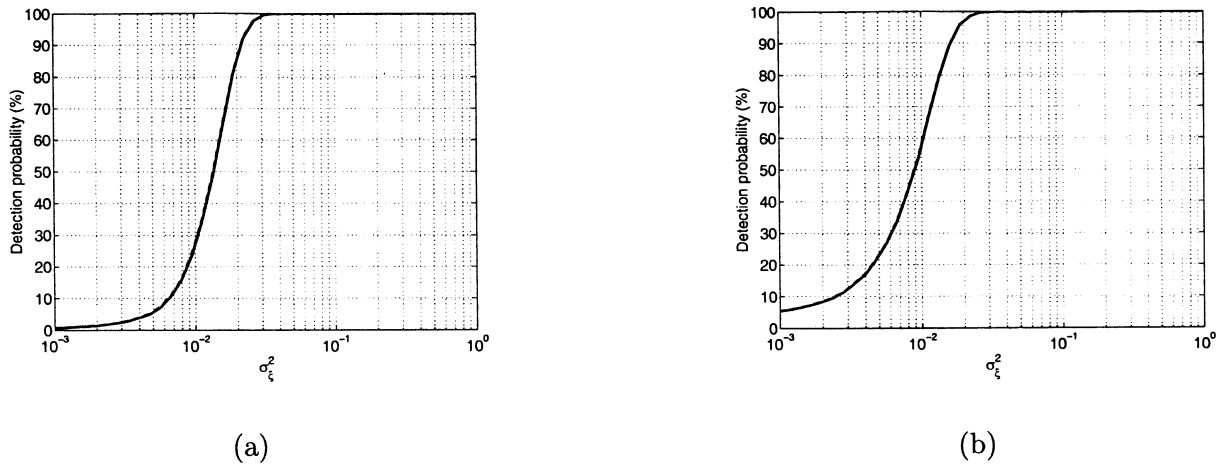

Fig. 2. Detection probability (in percent) of the SJA (solid) and NA (dashed) detectors in the presence of normally distributed jitter plotted against σ_ξ^2 with SNR = 10 dB and (a) $\alpha = 0.01$ and (b) $\alpha = 0.05$. The sample length $n = 512$.

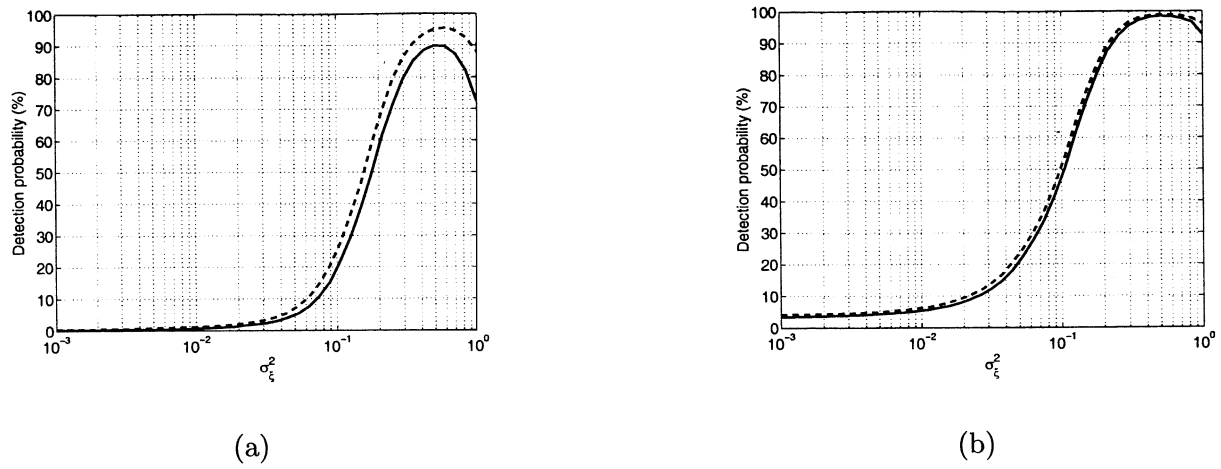

Fig. 3. Detection probability (in percent) of the SJA (solid) and NA (dashed) detectors in the presence of normally distributed jitter plotted against σ_ξ^2 with SNR = 0 dB, and (a) $\alpha = 0.01$ and (b) $\alpha = 0.05$. The sample length $n = 512$.

This can be computed using the asymptotic distribution results of Section II. Fig. 6 shows the sample length required for the SJA detector to achieve a detection probability of 95% plotted against σ_ξ^2 for several SNRs. The frequency $\omega_0 = 1$, the jitter is normally distributed, and the false alarm probability is 1%. It can be seen that once σ_ξ^2 decreases below a certain value,

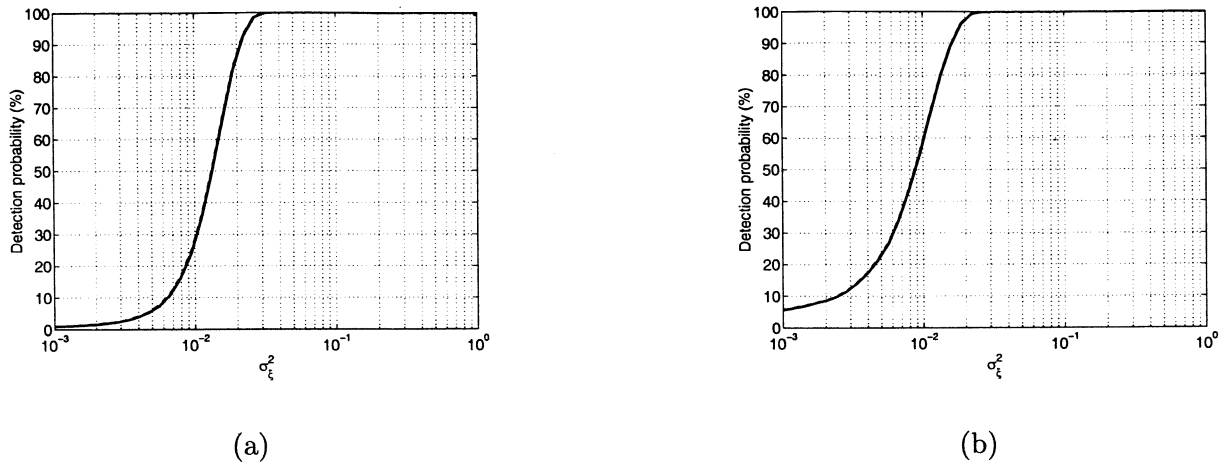

Fig. 4. Detection probability (in percent) of the SJA (solid) and NA (dashed) detectors in the presence of uniformly distributed jitter plotted against σ_ξ^2 with SNR $= 10$ dB and (a) $\alpha = 0.01$ and (b) $\alpha = 0.05$. The sample length $n = 512$.

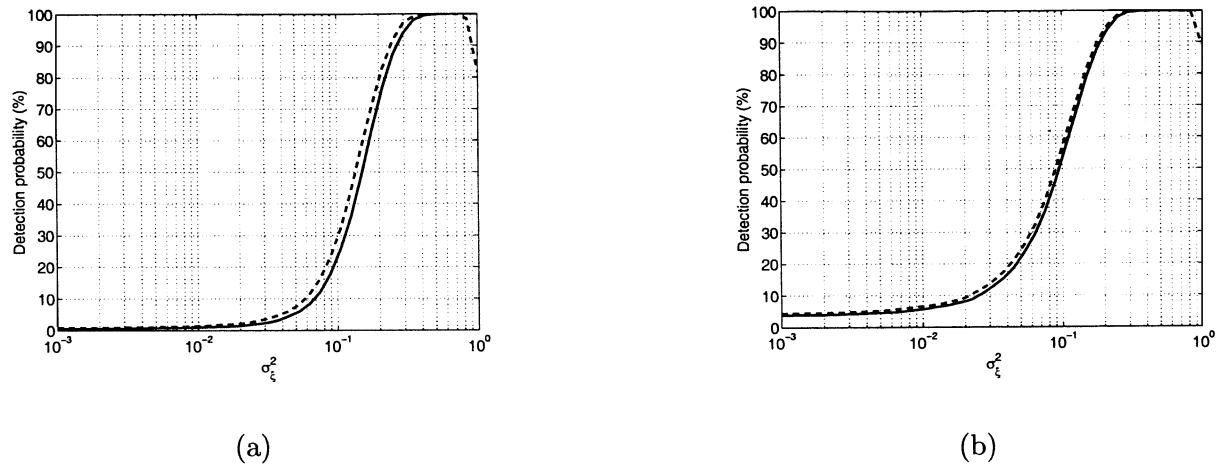

Fig. 5. Detection probability (in percent) of the SJA (solid) and NA (dashed) detectors in the presence of uniformly distributed jitter plotted against σ_ξ^2 with SNR $= 0$ dB, and (a) $\alpha = 0.01$ and (b) $\alpha = 0.05$. The sample length $n = 512$.

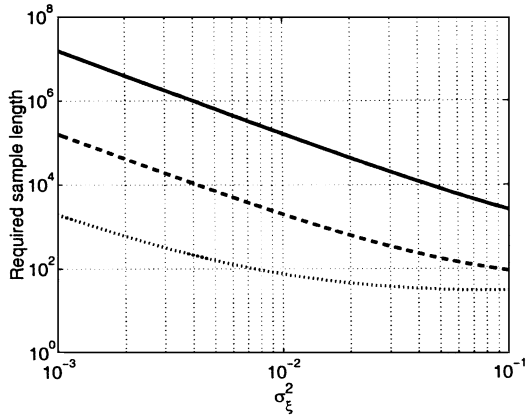

Fig. 6. Sample length required to achieve a detection probability of 95% plotted against σ_ξ^2 for SNR $= 0$ dB (solid), 10 dB (dashed), and 20 dB (dotted). The false alarm probability $\alpha = 0.01$.

say $c(\text{SNR})$, with dependence on the SNR indicated, the log of the required sample length increases linearly as the log of the jitter variance is decreased. Quantitatively, for $\sigma_\xi^2 < c(\text{SNR})$, a factor of 10 decrease in σ_ξ^2 causes a factor of 100 increase in the required sample length. For $\sigma_\xi^2 > c(\text{SNR})$, the required sample length is an almost constant function of σ_ξ^2. Similar results to those shown in Fig. 6 can be obtained for the NA detector and for uniformly distributed jitter.

IV. Conclusion

Two closely related methods were proposed for detecting the presence of symmetrically distributed independent timing jitter in a complex harmonic. One detector was obtained by employing a small jitter approximation, whereas the other was obtained through a normal assumption. The conditions required for consistency of the detectors were derived. Using these results, it was shown that the detectors are consistent for the important special cases of normally distributed jitter and uniformly distributed jitter, although mild conditions on the jitter variance apply for the case of uniformly distributed jitter. Simulation results showed that the small jitter approximation detector maintains the nominal false alarm probability in all cases, although it is excessively conservative for small sample lengths. The normal assumption detector does not maintain the set level for SNRs less than -3 dB, although the amount by which it exceeds the set level for these SNRs decreases as the sample length increases. The detectors exhibit good

performance under the alternative for relatively small sample lengths. The detectors performed similarly for high SNRs with differences in performance only becoming significant for low SNRs and large jitter variances.

This paper concentrated on detecting the presence of independent timing jitter. The problem of detecting accumulated timing jitter, which is correlated, is also worthy of study. Consequently, it is of interest to examine the detectors' performances in the presence of accumulated jitter.

APPENDIX A
DFT FREQUENCY AND PHASE ESTIMATORS

In this Appendix, we show that $\hat{\omega}_0 = \omega_0 + O_m(n^{-3/2})$ and $\hat{\psi} = \psi + O_m(n^{-1/2})$, where $\hat{\omega}_0$ and $\hat{\psi}$ are defined in (2) and (3), respectively, and the $O_m(\cdot)$ notation has been defined in Section II.

The signal (1) may be rewritten as

$$X_t = g_0\phi_\xi(1)\exp\{j(\omega_0 t + \psi)\} + \eta_t \tag{28}$$

where

$$\eta_t = g_0\{\exp(j\xi_t) - \phi_\xi(1)\} + W_t. \tag{29}$$

Equation (28) expresses the signal as a constant amplitude complex harmonic embedded in zero mean additive noise. Under the assumptions that $\eta_t = O_m(1)$ and $d_\eta^{(k)}(\omega_0) = O_m(n^{k+1/2}), k = 1, 2, \ldots$, where

$$d_\eta(\omega) = \sum_{t=0}^{n-1} \eta_t \exp(-j\omega t)$$

and $d_\eta^{(k)}(\omega)$ is the kth derivative of $d_\eta(\omega)$ with respect to ω, the frequency estimation error is [7, Lemma 1]

$$\hat{\omega}_0 - \omega_0 = 6\mathrm{Re}\left\{2d_\eta^{(1)}(\omega_0) - jnd_\eta^*(\omega_0)\right\}/\{g_0\phi_\xi(1)n^3\} + O_m(n^{-2}). \tag{30}$$

Clearly, $\eta_t = O_m(1)$ since W_t is normally distributed with finite variance and $\phi_\xi(k) = \mathsf{E}\exp(jk\xi_t) < \infty$ for $k = 1, 2, \ldots$. It remains to be shown that $d_\eta^{(k)}(\omega_0) = O_m(n^{k+1/2})$. We have that

$$d_\eta^{(k)}(\omega_0) = (-j)^k \sum_{t=0}^{n-1} t^k \eta_t \exp(-j\omega_0 t).$$

It is necessary to consider $\mathsf{E}\left|d_\eta^{(k)}(\omega_0)\right|^r$ only for r even as, by Jensen's inequality, $\mathsf{E}\left|d_\eta^{(k)}(\omega_0)\right|^r \le \sqrt{\mathsf{E}\left|d_\eta^{(k)}(\omega_0)\right|^{2r}}$. For r even, we have

$$\begin{aligned}
&\mathsf{E}\left|d_\eta^{(k)}(\omega_0)\right|^r \\
&= \sum_{t_1,\cdots,t_r=0}^{n-1} \mathsf{E}\prod_{i=1}^{r/2} t_i^k \eta_{t_i}\exp(-j\omega_0 t_i) \prod_{i=r/2+1}^{r} t_i^k \eta_{t_i}^*\exp(j\omega_0 t_i) \\
&\le \left[g_0^2\{1-\phi_\xi(1)^2\}+\sigma_W^2\right]^{r/2} \prod_{i=0}^{r/2-2}\binom{r-2i}{2}\left(\sum_{t=0}^{n-1} t^{2k}\right)^{r/2} \\
&= O(n^{rk+r/2})
\end{aligned}$$

Using this result and Jensen's inequality, we obtain $\mathsf{E}|d_\eta^{(k)}(\omega_0)/n^{k+1/2}|^r = O(1)$ for $r = 1, 2, \ldots$, so that $d_\eta^{(k)}(\omega_0)$ is $O_m(n^{k+1/2})$. Therefore, (30) holds, and $\hat{\omega}_0 = \omega_0 + O_m(n^{-3/2})$. We turn now to the phase estimator $\hat{\psi}$, which may be written as

$$\hat{\psi} = \mathrm{Im}\left[\log\left\{\sum_{t=0}^{n-1} X_t \exp(-j\hat{\omega}_0 t)\right\}\right]. \tag{31}$$

The demodulated signal $X_t\exp(-j\hat{\omega}_0 t)$ may be written as

$$\begin{aligned}
&X_t\exp(-j\hat{\omega}_0 t) \\
&\quad = \{g_0\exp(j\xi_t) + V_t\}\exp(j\psi)\exp\{-j(\hat{\omega}_0 - \omega_0)t\} \\
&\quad = \{g_0\exp(j\xi_t) + V_t\}\exp(j\psi)\exp\{1 - j(\hat{\omega}_0 - \omega_0)t \\
&\qquad + O_m(n^{-1})\}
\end{aligned} \tag{32}$$

where $V_t = W_t/\exp\{j(\omega_0 t + \psi)\}$, and we have used $\hat{\omega}_0 - \omega_0 = O_m(n^{-3/2})$. Substituting (32) into (31) gives

$$\hat{\psi} - \psi = \mathrm{Im}\log\{\gamma + \epsilon + O_m(n^{-1})\}$$

where

$$\gamma = \sum_{t=0}^{n-1} g_0\exp(j\xi_t)\{1 - j(\hat{\omega}_0 - \omega_0)t\} \tag{33}$$

$$\epsilon = \sum_{t=0}^{n-1} V_t\{1 - j(\hat{\omega}_0 - \omega_0)t\}. \tag{34}$$

Since $\gamma = O_m(n)$ and $\epsilon = O_m(n^{1/2})$, it can be shown that

$$\begin{aligned}
\hat{\psi} - \psi &= \mathrm{Im}(\gamma + \epsilon[2 - \gamma/\{ng_0\phi_\xi(1)\}])/\{ng_0\phi_\xi(1)\} \\
&\quad + O_m(n^{-1}) \\
&= \mathrm{Im}(\gamma + \epsilon)/\{ng_0\phi_\xi(1)\} + O_m(n^{-1})
\end{aligned} \tag{35}$$

where we have used $\mathrm{Im}(\epsilon\gamma) = \mathrm{Im}(\epsilon)\mathrm{Re}(\gamma) + O_m(n) = ng_0\phi_\xi(1)\mathrm{Im}(\epsilon) + O_m(n)$ since $\mathrm{Im}(\gamma) = O_m(n^{1/2})$. Since $\mathrm{Im}(\epsilon) = O_m(n^{1/2})$ and $\mathrm{Im}(\gamma) = O_m(n^{1/2})$, it follows from (35) that $\hat{\psi} = \psi + O_m(n^{-1/2})$, and the required result is obtained.

APPENDIX B
ALTERNATIVE SMALL JITTER APPROXIMATIONS

Restricting our attention to estimators that ensure a real-valued test statistic, the following variance estimators based on the small jitter approximation can be obtained as alternatives to $\tilde{\sigma}_\xi^2$ of (19):

$$\bar{\sigma}_\xi^2 = \frac{1 - (\hat{r}_{2Y} - \hat{\imath}_{2Y})/\hat{r}_Y^2}{2 - (\hat{r}_{2Y} - \hat{\imath}_{2Y})/\hat{r}_Y^2} \tag{36}$$

$$\check{\sigma}_\xi^2 = \hat{r}_Y^2/(\hat{r}_{2Y} - \hat{\imath}_{2Y}) - 1. \tag{37}$$

The test statistics $\bar{T} = \sqrt{n}\hat{r}_Y^2\bar{\sigma}_\xi^2/(2\hat{\imath}_{2Y})$ and $\check{T} = \sqrt{n}\hat{r}_Y^2\check{\sigma}_\xi^2/(2\hat{\imath}_{2Y})$ can be shown to be asymptotically standard normal under H. A simulation analysis shows that $\check{T}$ does not maintain the false alarm probability. The detector based on $\bar{T}$ maintains the nominal false alarm probability for all SNRs and sample lengths but has a smaller detection probability than the detector based on $\tilde{T}$. For this reason, we have proceeded in the analysis with $\tilde{T}$.

A different approach was used in [12] to derive an approximate maximum likelihood jitter variance estimator under the small jitter assumption for the real-valued sinusoid case. In [12], it is noted that the variance of $x_t = g_0\cos\{(\omega_0(t+u_t)+\psi\}+w_t$ at time index t can be approximated, using a first-order Taylor series expansion, by $\sigma_W^2+\sigma_U^2(s_t')^2$, where $s_t = g_0\cos(\omega_0 t+\psi)$, s_t' is the first derivative of s_t with respect to t, and the remaining notation is the same as that used for the complex-valued case. Since $s_t' = -\omega_0 s_t$, this leads to the variance approximation $\sigma_W^2+\omega_0^2\sigma_U^2 s_t^2$. The algorithm of [12] then applies the maximum likelihood procedure under the assumption that the residuals $(x_t - s_t) \sim N(0, \sigma_W^2+\omega_0^2\sigma_U^2 s_t^2), t = 0,\ldots,n-1$. Importantly, this is possible because the variance varies with time through the scaling of σ_U^2 by s_t^2. For the complex-valued case, the signal variance approximation becomes $\sigma_W^2+\sigma_U^2|s_t'|^2$ with $s_t = g_0\exp\{j(\omega_0 t+\psi)\}$. Substituting $s_t' = j\omega_0 s_t$ and noting that $|s_t|^2 = g_0^2$, we obtain $\sigma_W^2+g_0^2\omega_0^2\sigma_U^2$. Thus, under the small jitter assumption, the signal variance for a complex harmonic with jitter is constant with respect to time so that the approximate maximum likelihood algorithm of [12] cannot be applied.

Appendix C
Asymptotic Distribution of Moment Estimators

Let $\hat{\boldsymbol{\theta}} = (\hat{r}_Y, \hat{\imath}_{2Y}, \hat{r}_{2Y})', \boldsymbol{\theta} = (r_Y, \imath_{2Y}, r_{2Y})'$, and $\boldsymbol{\lambda} = (\lambda_1,\lambda_2,\lambda_3)'$, where λ_1, λ_2, and λ_3 are arbitrary real numbers. To find the asymptotic joint distribution of $\hat{\boldsymbol{\theta}}$, consider the scalar random variable

$$\begin{aligned}\zeta &= \sqrt{n}\boldsymbol{\lambda}'(\hat{\boldsymbol{\theta}}-\boldsymbol{\theta})\\ &= \sqrt{n}\{(\hat{r}_Y - r_Y)\lambda_1 + (\hat{\imath}_{2Y}-\imath_{2Y})\lambda_2 + (\hat{r}_{2Y}-r_{2Y})\lambda_3\}.\end{aligned}$$

Under the assumptions given in the Introduction

$$\mathrm{Re}(Y_t) = g_0\cos(\xi_t) + \mathrm{Re}(V_t) + O_m(n^{-1/2}) \tag{38}$$

$$\mathrm{Re}(Y_t)^2 = g_0\cos(\xi_t)^2 + 2g_0\mathrm{Re}(V_t)\cos(\xi_t) + \mathrm{Re}(V_t)^2 + O_m(n^{-1/2}) \tag{39}$$

$$\mathrm{Im}(Y_t)^2 = g_0\sin(\xi_t)^2 + 2g_0\mathrm{Im}(V_t)\sin(\xi_t) + \mathrm{Im}(V_t)^2 + O_m(n^{-1/2}). \tag{40}$$

The random process $\{V_t\} = W_t/\exp\{j(\omega_0 t+\psi)\}$ is probabilistically equivalent to $\{W_t\}$ since

$$\begin{aligned}\mathsf{E}(V_t)^k &= \mathsf{E}(W_t)^k\exp\{-jk(\omega_0 t+\psi)\} = 0 = \mathsf{E}(W_t)^k\\ \mathsf{E}(V_t)^k(V_t^*)^l &= \mathsf{E}(W_t)^k(W_t^*)^l\exp\{-j(k-l)(\omega_0 t+\psi)\}\\ &= \begin{cases}0, & k=l\\ k!\sigma_W^{2k}, & k\neq l\end{cases} = \mathsf{E}(W_t)^k(W_t^*)^l.\end{aligned}$$

Therefore, $\{V_t\}$ is a white normal random process. Since $\{\xi_t\}$ is also iid, it follows that $\mathrm{Re}(Y_t), \mathrm{Im}(Y_t)^2$, and $\mathrm{Re}(Y_t)^2$ are iid sequences, and, from the assumptions on U_t, and W_t, they have finite variance. Therefore, the Lindeberg–Lévy central limit theorem [8, p. 28] can be used to obtain

$$\zeta - \mu_\zeta \overset{a}{\sim} \mathsf{N}(0,\sigma_\zeta^2) \tag{41}$$

where μ_ζ and σ_ζ^2 are the mean and variance of ζ, which will be determined below.

It is straightforward to see that

$$\mathsf{E}\hat{r}_Y = g_0\phi_\xi(1) = r_Y \tag{42}$$

$$\mathsf{E}\hat{\imath}_{2Y} = \left[g_0^2\{1-\phi_\xi(2)\}+\sigma_W^2\right]/2 = \imath_{2Y} \tag{43}$$

$$\mathsf{E}\hat{r}_{2Y} = \left[g_0^2\{1+\phi_\xi(2)\}+\sigma_W^2\right]/2 = r_{2Y} \tag{44}$$

so that $\mu_\zeta = 0$. The variances and covariances can be found as

$$n\mathsf{var}(\hat{r}_Y) = \left[g_0^2\{1-2\phi_\xi(1)+\phi_\xi(2)\}+\sigma_W^2\right]/2 \tag{45}$$

$$n\mathsf{cov}(\hat{r}_Y,\hat{\imath}_{2Y}) = g_0^3\{2\phi_\xi(1)\phi_\xi(2) - \phi_\xi(1) - \phi_\xi(3)\}/4 \tag{46}$$

$$n\mathsf{cov}(\hat{r}_Y,\hat{r}_{2Y}) = g_0^3\{\phi_\xi(1)+\phi_\xi(3)-2\phi_\xi(1)\phi_\xi(2)\}/4 + g_0\sigma_W^2\phi_\xi(1) \tag{47}$$

$$n\mathsf{var}(\hat{\imath}_{2Y}) = g_0^4\{1-2\phi_\xi(2)^2+\phi_\xi(4)\}/8 + g_0^2\sigma_W^2\{1-\phi_\xi(2)\}+\sigma_W^4/2 \tag{48}$$

$$n\mathsf{cov}(\hat{\imath}_{2Y},\hat{r}_{2Y}) = -g_0^4\{1-2\phi_\xi(2)^2+\phi_\xi(4)\}/8 \tag{49}$$

$$n\mathsf{var}(\hat{r}_{2Y}) = g_0^4\{1-2\phi_\xi(2)^2+\phi_\xi(4)\}/8 + g_0^2\sigma_W^2\{1+\phi_\xi(2)\}+\sigma_W^4/2. \tag{50}$$

Using (45)–(50) gives

$$\begin{aligned}\sigma_\zeta^2 = n\{&\lambda_1^2\mathsf{var}(\hat{r}_Y) + 2\lambda_1\lambda_2\mathsf{cov}(\hat{r}_Y,\hat{\imath}_{2Y})\\ &+2\lambda_1\lambda_3\mathsf{cov}(\hat{r}_Y,\hat{r}_{2Y}) + \lambda_2^2\mathsf{var}(\hat{\imath}_{2Y})\\ &+2\lambda_2\lambda_3\mathsf{cov}(\hat{\imath}_{2Y},\hat{r}_{2Y}) + \lambda_3^2\mathsf{var}(\hat{r}_{2Y})\}.\end{aligned} \tag{51}$$

It follows from (41), (51), and the Cramér-Wold device [8, Th. 1.5.2] that

$$\sqrt{n}(\hat{\boldsymbol{\theta}}-\boldsymbol{\mu}_{\hat{\boldsymbol{\theta}}}) \overset{a}{\sim} \mathsf{N}(0,\boldsymbol{\Sigma}_{\hat{\boldsymbol{\theta}}}) \tag{52}$$

where $\boldsymbol{\mu}_{\hat{\boldsymbol{\theta}}} = \mathsf{E}\hat{\boldsymbol{\theta}}$, and $\boldsymbol{\Sigma}_{\hat{\boldsymbol{\theta}}} = n\mathsf{E}(\hat{\boldsymbol{\theta}}-\boldsymbol{\mu}_{\hat{\boldsymbol{\theta}}})(\hat{\boldsymbol{\theta}}-\boldsymbol{\mu}_{\hat{\boldsymbol{\theta}}})'$. The elements of $\boldsymbol{\mu}_{\hat{\boldsymbol{\theta}}}$ are given by (42)–(44), and the elements of $\boldsymbol{\Sigma}_{\hat{\boldsymbol{\theta}}}$ are given by (45)–(50).

References

[1] S. S. Awad, "The effects of accumulated timing jitter on some sine wave measurements," *IEEE Trans. Instrum. Meas.*, vol. 44, pp. 945–951, Oct. 1995.

[2] S. S. Awad and M. F. Wagdy, "More on jitter effects on sinewave measurements," *IEEE Trans. Instrum. Meas.*, vol. 40, pp. 549–552, June 1991.

[3] A. Berkovitz and I. Rusnak, "FFT processing of randomly sampled harmonic signals," *IEEE Trans. Signal Processing*, vol. 40, pp. 2816–2819, Nov. 1992.

[4] E. R. Dowski, C. A. Whitmore, and S. K. Avery, "Estimation of randomly spaced sinusoids in additive noise," *IEEE Trans. Acoust., Speech, Signal Processing*, vol. 36, pp. 1906–1908, Dec. 1988.

[5] H. Hofer, P. Artal, B. Singer, J. L. Aragón, and D. R. Williams, "Dynamics of the eye's wave aberration," *J. Opt. Soc. Amer.*, vol. 18, no. 3, pp. 497–506, Mar. 2001.

[6] J. Liang, B. Grimm, S. Goelz, and J. F. Bille, "Objective measurement of wave aberrations of the human eye with the use of a Hartmann-Shack wavefront sensor," *J. Opt. Soc. Amer.*, vol. 11, no. 7, pp. 1949–1957, 1994.

[7] B. Porat and B. Friedlander, "Asymptotic statistical analysis of the high-order ambiguity function for parameter estimation of polynomial-phase signals," *IEEE Trans. Inform. Theory*, vol. 42, pp. 995–1001, June 1996.

[8] R. J. Serfling, *Approximation Theorems of Mathematical Statistics*. New York: Wiley, 1980.

[9] I. Sharfer and H. Messer, "The bispectrum of sampled data: Part 1—Detection of the sampling jitter," *IEEE Trans. Signal Processing*, vol. 41, pp. 296–312, Jan. 1993.

[10] ——, "The bispectrum of sampled data: Part 2—Monte Carlo simulations of detection and estimation of the sampling jitter," *IEEE Trans. Signal Processing*, vol. 42, pp. 2706–2714, Oct. 1994.
[11] D. N. Swingler, "Approximations to the Cramér-Rao lower bound on frequency estimates for complex sinusoids in the presence of sampling jitter," *Signal Process.*, vol. 48, pp. 77–83, 1996.
[12] G. Vandersteen and R. Pintelon, "Maximum likelihood estimator for jitter noise models," *IEEE Trans. Instrum. Meas.*, vol. 49, pp. 1282–1283, Dec. 2000.
[13] M. F. Wagdy and S. S. Awad, "Effect of sampling jitter on some sine wave measurements," *IEEE Trans. Instrum. Meas.*, vol. 39, pp. 86–89, Feb. 1990.
[14] K. M. Wong, R. S. Walker, and G. Niezgoda, "Effects of random sensor motion on bearing estimation by the MUSIC algorithm," *Proc. Inst. Elect. Eng. F*, vol. 135, no. 3, pp. 233–250, June 1988.

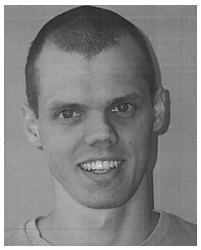

Mark R. Morelande received the B.Eng. degree in aerospace avionics from Queensland University of Technology (QUT), Brisbane, Australia, in 1997 and the Ph.D. degree in electrical engineering from Curtin University of Technology, Perth, Australia, in 2001.

From November 2000 to January 2002, he was a Postdoctoral Fellow with the Centre for Eye Research, QUT. Since January 2002, he has been a Research Fellow with the Cooperative Research Centre for Sensor, Signal, and Information Processing, University of Melbourne, Parville, Australia. His research interests include nonstationary signal analysis and target tracking with particular emphasis on multiple target tracking and the application of sequential Monte Carlo methods to tracking problems.

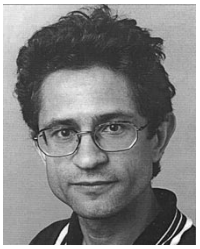

D. Robert Iskander (M'98) received the Magister Inżynier degree in electronic engineering from the Technical University of Lodz, Lodz, Poland, in 1991 and the Ph.D. degree in signal processing from Queensland University of Technology (QUT), Brisbane, Australia, in 1997.

From 1996 to 1998, he was a Post-Doctoral Fellow with the Signal Processing Research Centre and the Cooperative Research Centre for Satellite Systems, QUT, and from 1998 to 2000, he was a Research Fellow with the Centre for Eye Research, QUT. In 2001, he joined the School of Engineering, Griffith University, Gold Coast, Australia, as a Senior Lecturer. In July 2003, he returned to the Centre for Eye Research as a Principle Research Fellow. His current research interests include statistical signal processing, visual optics, and optometry.

Dr. Iskander is a member of the Association for Research in Vision and Ophthalmology and an Honorary Fellow at Griffith University.